

# EXPLOITATION OF NONLINEAR EFFECTS FOR ENHANCEMENT OF THE SENSING PERFORMANCE OF RESONANT SENSORS

Seungkeun Choi, Seong-Hyok Kim, Yong-Kyu Yoon\* and Mark G. Allen

School of Electrical and Computer Engineering  
Georgia Institute of Technology, Atlanta, GA 30332 USA  
Email: gtg737d@mail.gatech.edu

**Abstract:** Nonlinear effects in resonating structures have been exploited to achieve high sensing performance. The nominal platform consists of a disc type resonant magnetic sensor, comprising a permanent magnet supported by multiple micromachined silicon beams. Nonlinearity effects on sensitivity have been characterized as a function of beam width and the number of beams using analytical models as well as numerical analysis. By increasing the number of beams while reducing beam width (and thereby maintaining constant nominal linear resonant frequency), large nonlinearity has been obtained, resulting in increased change in operating resonant frequency per unit applied magnetic field. To verify the result experimentally, magnetic sensors with differing beam dimensions are microfabricated and tested. As expected, a structure with 6 beams and a beam width of  $13.1 \mu\text{m}$  shows a higher normalized sensitivity of  $0.196 \text{ [mHz/Hz}\cdot\text{degree]}$  than one with 4 beams and a beam width of  $14.6 \mu\text{m}$  of  $0.086 \text{ [mHz/Hz}\cdot\text{degree]}$  in detection of the direction of the magnetic field of the earth.

**Keywords:** FEM simulation, magnetic sensor, MEMS, nonlinear effects, resonant sensors.

## 1. INTRODUCTION

MEMS-based mechanically-resonant sensors, in which the sensor resonant frequency shifts in response to the measurand, are widely utilized [1]. Such sensors are typically operated in their linear resonant regime. However, substantial improvements in resonant sensor performance (functionally defined as change in resonant frequency per unit measurand change) can be obtained by designing the sensors to operate far into their nonlinear regime. This effect is illustrated through the use of a magnetically-torqued, rotationally-resonant MEMS platform. Platform structural parameters such as beam width and number of beams are parametrically varied subject to the constraint of constant small-deflection resonant frequency.

In this research, a mechanical resonator is employed as a sensing element to measure the direction of the Earth's magnetic field. The test structure consists of a mechanically-resonant silicon platform supported by varying numbers and geometries of silicon beams and bearing a

permanent magnet. The interaction between an external magnetic field  $H$  and the magnet magnetization  $M$  generates a torque that changes the effective stiffness of the beam, resulting in a change of the resonant frequency ( $f$ ) of the sensor (Fig. 1 (a)).

This structure has been previously demonstrated as a magnetic sensor [2, 3]. The resonator with electromagnetic sensing and excitation coils is hybrid integrated with self-oscillation electronics and gives a resonant frequency shift as a function of the strength and orientation changes of the external magnetic field  $H$ . Here, we explore the use of design choices to drive the sensor more deeply into its nonlinear regime in order to assess the potential for performance improvement.

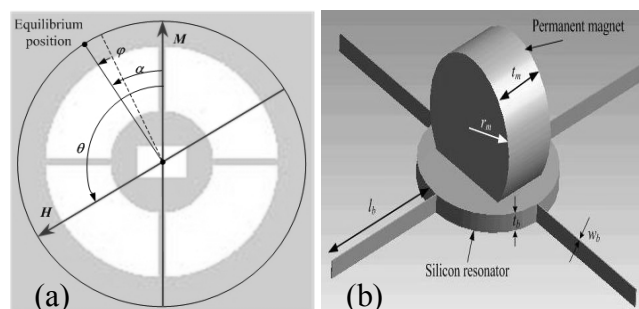


Fig. 1 Images of mechanical resonator. (a) Device concept, (b) Structural parameters.

\*Present address: Department of Electrical Engineering, State University of New York, Buffalo, NY 14260 USA

## 2. THEORETICAL MODELING

Since the deflections of the beams may be large compared with their widths, geometric nonlinearity effects must be taken into account to obtain an analytical expression of the resonant frequency of the device as a function of the amplitude and direction of the external field [2]. When the magnetization and the magnetic field are not perfectly aligned, the center disk rotates by an angle  $\alpha$  that depends primarily on  $k_l$  and  $T_0$  (Fig. 1 (a)). This angle is determined by solving the static equilibrium equation:

$$k_l \alpha + k_{nl} \alpha^3 - T_0 \sin(\theta - \alpha) = 0 \quad (1)$$

where  $T_0$  is the magnitude of the torque generated from the magnet,  $I$  is the platform moment of inertia,  $\theta$  is the angle between the external magnetic field and the magnetization of the magnet, and  $k_l$  and  $k_{nl}$  are the linear and nonlinear stiffness coefficients.

The maximum amplitude of the magnetic torque,  $T$ , is given by Eq. 2 for a permanent magnet of volume  $V$  and magnetization  $M$ .

$$T_0 = \mu_0 M \cdot V \cdot H \quad (2)$$

Assuming a single degree of freedom torsional vibratory system, the expression of the fundamental resonant frequency of the sensor is obtained by solving the differential equation satisfied by the angle of vibration,  $\varphi$ :

$$I \ddot{\varphi} + k_l(\alpha + \varphi) + k_{nl}(\alpha + \varphi)^3 = T_0 \sin(\theta - (\alpha + \varphi)) \quad (3)$$

For small oscillation angles, the resonant frequency of the system is:

$$f^2 = (1/4\pi^2)((k_l + 3k_{nl}\alpha^2 + T_0 \cos(\theta - \alpha))/I) \quad (4)$$

Since the value of  $\alpha$  depends on  $\theta$ , a maximum frequency shift for a given  $k_l$  is obtained when  $k_{nl}$  is maximized (Eq. 4). This maximization can occur through geometric design of the support beams (Fig. 1 (b)).

A narrow beam width is preferred for high sensing performance since it makes the resonator more sensitive to the external environmental. However, if beam width is too thin compared to other geometric parameters, the resonator becomes mechanically weak; this can be compensated for by increasing the number of beams to bring the linear stiffness back to its original value. Adjustment of beam width with and without compensation is investigated.

As the beam width decreases, the numerical values of the  $k_l$  and  $k_{nl}$  decrease (Table.1), resulting in an increment of  $\alpha$  at a given torque (Eq.1). Therefore, the magnitude of  $3k_{nl}\alpha^2$  becomes larger as the beam width decreases while there is no change for  $T_0 \cos(\theta - \alpha)$ . Even though the nonlinear stiffness decreases as the beam width decreases, the term  $k_{nl}\alpha^2$  increases as the beam width decreases since the increasing rate of the  $\alpha^2$  is faster than the decreasing rate of the  $k_{nl}$ . Therefore, the normalized sensitivity decreases/increases as the beam width increases/decreases when the same numbers of beams are used. The normalized sensitivity also increases with a larger external magnetic field since the equilibrium angle,  $\alpha$ , becomes larger with increasing external magnetic field at a given  $k_l$  and  $k_{nl}$  (Table1). In addition, when the linear stiffness is determined, the sensitivity is maximized by increasing the nonlinearity which can be achieved by adding more beams while decreasing beam width.

Table 1. Normalized sensitivity from the theoretical characterizations. Normalized sensitivity is defined as the amount of resonant frequency shift per unit rotational angle divided by the resonant frequency at  $\theta=0$ .

$N_b$ (Number of beams)	$w_b$ [ $\mu\text{m}$ ]	$k_l$ [ $10^{-6}$ Nm]	$k_{nl}$ [ $10^{-2}$ Nm]	Normalized sensitivity [mHz/(Hz·degree)]		
				50 $\mu\text{T}$	0.195 mT	1.95 mT
4	10	16.56	9.12	1.5	21.5	27.8
	20	132.13	18.70	0.0112	2.0	4.88
	30	445.48	31.60	0.00094	0.11	0.44
8	15.88	132.28	29.1	0.0153	2.756	6.157
16	12.61	132.47	46.2	0.022	3.727	7.659

The width of beam is selected such that the linear stiffness coefficients are the same for different number of beams. There is not much effect on  $\alpha$  since the  $k_l$  is set to be equal, thereby  $3k_{nl}\cdot\alpha^2$  becomes large as  $k_{nl}$  increases. The difference between the maximum and minimum resonant frequencies normalized by the minimum resonant frequency is taken as a measure of sensor performance. As shown in Table1,  $k_{nl}$  increases as the beam width decreases even though more beams are used to keep the linear stiffness constant, increasing the normalized sensitivity.

### 3. FINITE ELEMENT SIMULATION

A parametric study of geometric nonlinearity maximization is carried out by using ANSYS to determine the linear and nonlinear spring constants for a variety of beam geometries (Fig. 2), and solving Eqs. (1) ~ (4) to determine the system resonant frequency as a function of external magnetic field angle  $\theta$ . Typical ANSYS results are shown in Fig. 3, from which spring constants are extracted (Table 2). As beam width decreases, the numerical values of  $k_l$  and  $k_{nl}$  decrease. However,  $k_{nl}$  decreases far more slowly than  $k_l$ . Therefore, the normalized performance increases as the beam width decreases for a fixed number of beams. Alternatively, when the linear stiffness is held constant, sensor performance is maximized by increasing the nonlinearity of the resonator. Maximum sensitivity would therefore be achieved by having an infinite number of beams of vanishingly small width. However, the minimum width of beam is limited due to the aspect ratio limitation of the fabrications

### 4. FABRICATION AND MEASUREMENT

Resonators of differing beam width and number, but the same nominal  $k_l$ , are fabricated and characterized at various external magnetic fields. Although the three-beam and four-beam structures were reasonably well-matched, fabrication discrepancies led to the  $k_l$  of the six-beam structures not being exactly matched.

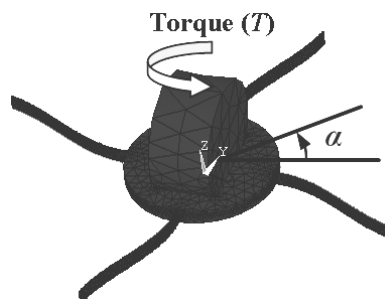


Fig. 2 Structure for ANSYS simulation.

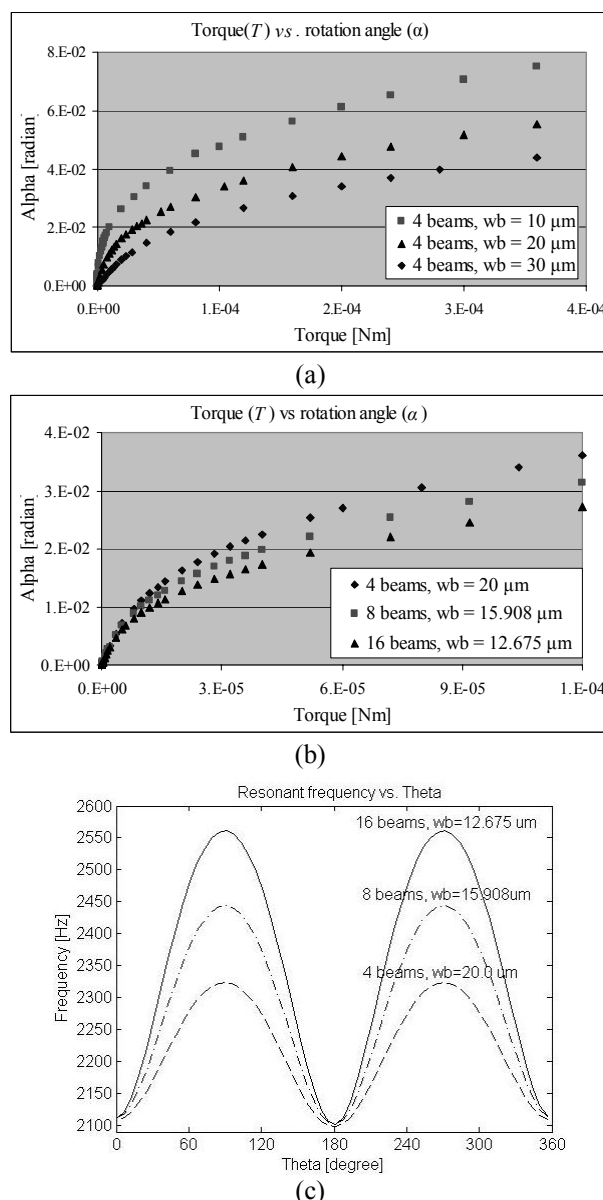


Fig. 3 ANSYS results. (a) Torque vs. rotational angle of different beam width for 4 beam structure, (b, c) Torque vs. rotational angle and the resonant frequency curves of different combinations of beam width and number of beams, respectively (applied field of 1.95 mT).

Table 2. Normalized sensitivity from the ANSYS simulations.

$N_b$ (Number of beams)	$w_b$ [ $\mu\text{m}$ ]	$k_l$ [ $10^{-6}$ Nm]	$k_{nl}$ [ $10^{-2}$ Nm]	Normalized sensitivity [mHz/(Hz·degree)]		
				50 $\mu\text{T}$	0.195 mT	1.95 mT
4	10	73.3	83.8	0.1	11.44	17.63
	20	581.0	191.96	0.0018	0.320	1.130
	30	1936.7	320.2	0.0002	0.012	0.055
8	15.908	586	333.2	0.0024	0.532	1.7466
16	12.675	594	517.6	0.0031	0.768	2.361

Both three and four beam structures show higher performance as the beam width decreases (Table3, Fig.4). Although the frequencies were not exactly matched, the six beam structure showed higher normalized performance at all the measured external magnetic fields as expected (Table4, Fig.5), demonstrating the beneficial effects of nonlinear maximization.

confirmed with measurement result from the magnetically-torqued and rotationally-resonant MEMS platform. Characterization results provide a useful way to enhance sensing performance of the resonant-based sensors by maximizing structural nonlinearity.

Table 3. Normalized sensitivity from the measurements (Beam width characterization).

$N_b$	$w_b$ [ $\mu\text{m}$ ]	$f_c$ [Hz]	Normalized sensitivity [mHz/(Hz·degree)]	
			0.975 mT	1.95 mT
3	17.2	1580	1.169	2.969
	21.2	2102	0.122	0.538
4	15.6	1498	1.142	3.319
	21.4	2493	0.067	0.323

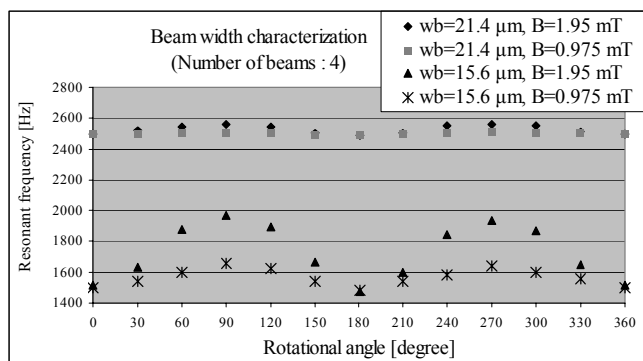


Fig. 4 Resonant frequency measurement with different beam width for 4 beam structure.

Table 4. Normalized sensitivity from the measurements (characterization of the beam width and number of beams).

$N_b$	$w_b$ [ $\mu\text{m}$ ]	$f_c$ [Hz]	Normalized sensitivity [mHz/(Hz·degree)]		
			Earth field	0.195 mT	0.39 mT
4	14.6	1248.3	0.086	0.192	0.431
6	13.1	1437.5	0.196	0.509	0.876

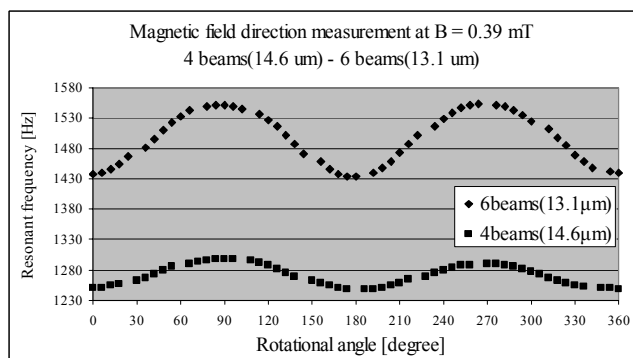


Fig. 5 Resonant frequency measurement for 4 beam and 6 beam structures.

### 5. CONCLUSIONS

Nonlinear performance improvement characterization is performed both analytically as well as with FEM simulation. The theory was

### REFERENCES

[1] O. Brand, "CMOS-based resonant sensors," *IEEE Sensors*, pp. 129-132, 2005.  
 [2] T. C. Leichle, M. Von Arx, S. Reiman, I. Zana, W. Ye, and M. G. Allen, "A low-power resonant micromachined compass," *J. Micromech. Microeng.* v. 14, p. 462-70, 2004.  
 [3] S. Choi, S.-H. Kim, Y.-K. Yoon, and M. G. Allen, "A magnetically excited and sensed MEMS-based resonant compass," *IEEE Trans. Mag.*, vol. 42, pp. 3506-08, 2006